Carpathian Journal of Earth and Environmental Sciences, February 2015, Vol. 10, No. 1, p. 27 - 39

CLAY MINERALS-CLINOPTILOLITE ASSEMBLAGES IN TWO ROMANIAN TUFFS

Ramona BALINT[1,2,*], Laura-Gabriela CALOTESCU[1], Valter BOERO[1] & Franco AJMONE-MARSAN[1]

[1]*DISAFA. – Chimica Agraria, Università degli Studi di Torino, Largo Paolo Braccini 2, 10095, Grugliasco, Torino, Italy, valter.boero@unito.it, franco.ajmonemarsan@unito.it*

[2]*Geological Institute of Romania, Str. Caransebes nr.1, Sector 1, 012271, Bucureşti, Romania; balint.ramona@yahoo.com*

Abstract: Mineral samples from two Miocene tuff deposits from Romania (Goleşti and Slănic) were studied in order to understand which parameters may control the mineral assemblage. Both acidic tuffs were formed of kaolinite, minerals of the illite/smectite series (R0 illite/smectite and illite), clinoptilolite, alkali feldspars and SiO_2 phases. The characterization of clay and zeolite minerals and the percentage of smectite layers in R0 illite/smectite suggest that the formation of R0 illite/smectite at Goleşti occurred directly from volcanic glass, while at Slănic it could be the result of the smectite illitization. The percentage of smectite layers and the comparative clay minerals/clinoptilolite ratio would indicate that the two deposits might have had different evolutions. Phase transformation at Goleşti potentially proceeded at a relatively low depth, suffering an important chemical control, while at Slănic the authigenesis suggests a greater formation depth and a weaker chemical control. Therefore, the two deposits may depict different alteration degrees of the same volcanic glass.

Keywords: zeolite, clinoptilolite, clay minerals, Miocene volcanic glass, authigenesis, illite, smectite.

1. INTRODUCTION

Volcanic glass forming under high pressure and temperature conditions becomes thermodynamically unstable under surface conditions. Its further evolution depends on several factors, such as glass and solution composition, depth, and temperature. Natural occurrences and experimental research studies have shown, however, that the secondary minerals that generally form in most glass-solution systems are alumino-silicatic gels, clay minerals, zeolites, alkali feldspars and SiO_2 phases (de'Gennaro et al., 2000).

Dibble & Tiller (1981) suggested that the paragenesis of tuffaceous sediments does not reflect a thermodynamic equilibrium. In fact, the mineral assemblage is metastable, consisting of phases with the highest nucleation rate, able to decrease more quickly the free energy of the bulk system. According to Oswald's rule, the crystallization sequence generally starts from the most disordered and less stable phases (alumino-silicatic gels), and progresses to more stable and ordered phases, until equilibrium is reached. Moreover, the sequential natural assemblage is mainly controlled by the phases with highest growing rates, which include the majority of network formers. However, other phases with slower growing rates may simultaneously form. Therefore, a metastable authigenic assemblage resulting from glass-solution systems may occur as a sequence of metastable phases reflecting the general evolution trend of the system, or as an association of both dominant and subordinated phases, simultaneously formed.

System genesis and evolution may be elucidated by studying the occurrences and structural and chemical features of two groups of authigenic phases, namely clay minerals and zeolites, even if present in small amounts. The most common clay minerals found both in natural occurrences and in experimental works, following acidic glass alteration are kaolinite, smectite, illite/smectite, and illite, while the most common zeolites are clinoptilolite, mordenite and analcime (Neuhoff & Ruhl, 2006). Clay minerals-zeolites assemblages are influenced by the geological conditions of the natural systems (volcanism type, depositional system, and diagenesis) which affect

glass and water chemistry, and their formation depth and temperature. However, it is difficult to establish a univocal correlation between the crystallization sequence and the geological evolution, since little information on natural occurrences or experimental results is available for similar systems.

Smectite is usually considered the first phase which crystallizes in natural occurrences where the mineral assemblages include clay minerals and zeolites, being replaced by clinoptilolite and illite as alteration progresses. In fact, Cerri et al., (2001) suggested that the early stage of alteration could be dominated by the transformation of glass matrix into smectite, followed by clinoptilolite crystallization at higher pH, due to an extensive or total dissolution of the glass shards. Broxton et al., (1987) indicated that smectite potentially form either within deep or moderately deep sediments, where the pH is 7-9. In their study, however, smectite did not appear to be replaced by clinoptilolite, but suffered a direct transition to illite/smectite, which could be justified by a higher geothermal gradient. Nevertheless, an anomalous association between smectite and clinoptilolite was also observed by Ghiara et al., (2000) in several deposits from Sardinia where, in most samples, smectite seemed to have formed before clinoptilolite. However, in some mineral assemblages, smectite appeared on the corroded clinoptilolite, probably due to sudden changes of interacting fluids.

Experimental works on volcanic glass alteration provided better explanation for the crystallization sequence and processes which lead to clay minerals and zeolite authigenesis. For example, according to Barth-Wirsching & Höller (1989), smectite usually does not occur in closed systems where zeolites represent the dominant phase. Ghiara & Petti (1996) stated that the $[Na^+ + K^+]/[H^+]$ ratio and SiO_2 activity are the major parameters controlling the crystallization sequence for clay minerals and zeolites, with simultaneous crystallization occurring at fluid pH>9.

Other experimental research carried out by de'Gennaro et al., (1988, 1993) on trachytic glass alteration into saline solutions and deionized water described mineral assemblages consisting mainly of smectite, illite, zeolites and feldspars. Smectite and zeolites occurred in all systems and represented the prevalent phases, while illite crystallized in moderate amounts only in systems with saline solutions. Illite crystallization was promoted by the contemporary high availability of K and six-fold coordinated Al, which further causes the depletion of smectite. Therefore, illite may form either by direct precipitation or by smectite transformation. In most experiments, smectite and illite were found as single secondary phases, while other studies described a mixed-layer illite/smectite mineral association. The latter may result directly from glass alteration (Cerri et al., 2001; de la Fuente et al., 2000; Zevenbergen et al., 1996) or could form by illitization of previously formed smectite (Amouric & Olives, 1991; Anjos, 1986; Broxton et al., 1987).

Several studies describing the occurrences of secondary mineral assemblages in the Eastern and Western Carpathians are available (Miron et al., 2012; Damian et al., 2007; Cochemé et al., 2003), giving particular insight into the environmental effects of clay mineral alteration (Stumbea, 2010) or use of zeolites for environmental remediation (Balint et al., 2014; Pop et al., 2012; Nimirciag, 2012). Less attention has been given to the clay minerals-clinoptilolite assemblages from the Southern Carpathians. The aim of this study is to understand the genesis and paragenesis of two Romanian pyroclastic deposits of clay minerals and clinoptilolite formed in the Southern Carpathians by alteration of an acidic volcanic glass.

2. MATERIALS AND METHODS

2.1. Occurrence and geological setting

The pyroclastic deposits from Slănic-Prahova (SL) are located in the curvature zone of the Eastern Carpathians, in the Tarcău Unit; the deposits from Goleşti (GO) are located in the Southern Carpathians, within the Getic Depression (Fig. 1).

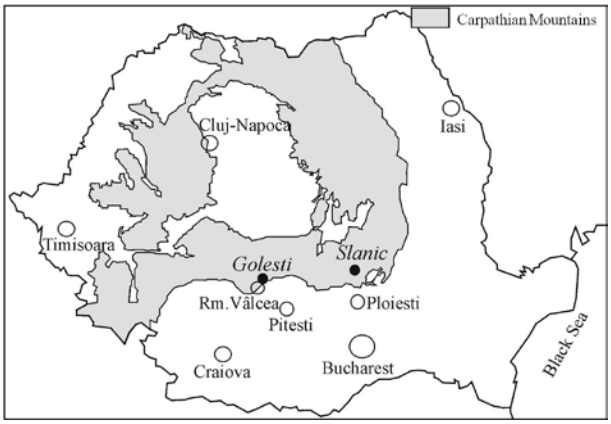

Figure 1. Location of Goleşti and Slănic deposits in Romania.

Both occurrences are related to the Medium Miocene deposits, described as "tuff with Globigerines". The SL tuff (50-150 m thick) lies in the post-tectonic cover units of the Lower Miocene tectogenesis, in a synclinal structure (10.5 km along the axis and 1.5-4.5 km perpendicularly). The synclinal filling consists of Medium Miocene

deposits (salts and breccia, shales with Radiolars and marls with Spirialis) with a maximum thickness of 1400 m (Fig. 2a). This region has undergone a complex polyphasic tectonic evolution, which resulted in an almost vertical position of the synclinal borders (inclination ~60°). The GO tuff lies in a region with simpler tectonics, in a vast monoclinal structure, part of Govora-Ocnele Mari mega-anticlinal, which covers an area of 31 km W-E and maximum 8.6 km N-S. The pyroclastic stratum has variable thickness, in some regions reaching more than hundred meters. The GO tuff is almost horizontal (inclination ~15°), with an average thickness of 110 m (Fig. 2b). The covering epiclastic and evaporitic sediments (Medium-Upper Miocene and Pliocene) are 185 m thick.

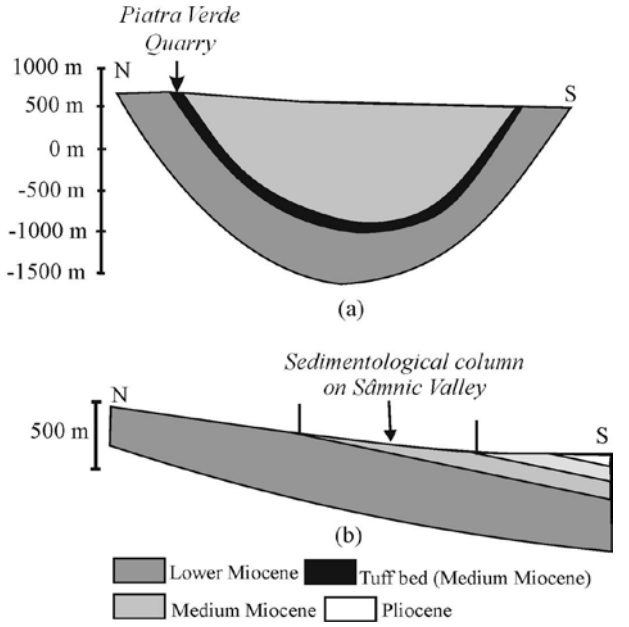

Figure 2. Transversal section of the deposits: (a) Slănic; (b) Goleşti.

Both pyroclastic deposits consist of lutitic-arenitic rocks in a sequence of predominantly volcanogenic material, and minor epiclastic formations in the same layer or in alternation. Similar volcanological and sedimentological features have been previously reported (Istrate, 1980). Observations on the glass shard morphology indicate a subaerian explosion for SL and a phreato-magmatic or submarine explosion for GO. The pyroclastic material appears to have undergone a mass transport and, on short distances, was probably transported in suspension or by traction. The depositional rates for both tuffs would have been generally high, in spite of the presence of some lutitic layers with elevated Globigerines contents, typical of a slow sedimentation in shelf region, under tempest waves level. However, some differences between the sedimentary structures occur, since diagenetical and depositional formations prevail in SL and GO, respectively.

2.2. Analytical techniques

Samples were collected from two sedimentological columns of each deposit. The column sampled at SL is located at the surface of Piatra Verde quarry, in the northern part of the synclinal, with a N-S direction (Fig. 2a). The column studied at GO has a N-S direction and is located along the Sâmnic Valley (Fig. 2b). Preliminary analysis on petrographic features, bulk mineralogical and chemical composition (optical microscopy and instrumental determinations) were performed on 25 samples from SL and 40 samples from GL.

Four samples containing both clay minerals and zeolites were collected from different depths of each deposit for further analysis. In order to investigate the authigenic clay minerals, the <0.2 μm fraction was separated. The samples collected from SL were named 24bs, 49bs, 38bs and 43bs, while those from GL were 20vg, 49vg, 47vg and 31vg.

The chemical composition of bulk samples (major and trace elements) was determined by X-ray fluorescence spectrometry (XRF, Philips PW1404), and their mineralogical composition identified by X-ray powder diffraction (XRD, Siemens D-5000 Kristalloflex diffractometer), using: CuKα radiation, step width 0.02° 2θ, scanning time 4 sec/step.

Mineralogical characterization of the <0.2 μm fraction was carried out by XRD analysis (Philips PW1710), using the following operative conditions: CoKα radiation, 1° divergence slit and 2° receiving slit, 3-60°2θ Co range, 0.01°2θ step, 10 sec counting time (Środoń, 1980). Oriented clay mineral samples for XRD traces were prepared from previously dialized suspensions. The XRD data were collected from untreated, air-dried samples and from Na-exchanged, ethylene glycol-solvated specimens. Further analysis (3-35°2θ Co, 0.02°2θ step, 4 sec/step counting time) on previously heated samples (550 °C, 1 h) were performed in order to differentiate kaolinite from Fe-rich chlorite (Moore & Reynolds Jr., 1997). All samples were chemically pretreated to eliminate carbonates, following the procedure described by Rabenhorst & Wilding (1984), using NaOAc buffer, pH 4.5. The <0.2 μm fraction was exchanged with Na according to the method elaborated by Moore and Reynolds Jr. (1997); salts were removed by dialysis. Glycolated samples were prepared by pressing on a filter paper wet with ethylene glycol for 24 hours (Środoń, 1980).

Table 1. Sample position and description.

Samples		Depth (m)		Layer thickness (m)	Description
		within the pyroclastites stratum	within the actual sedimentary column		
Slănic	24bs	14	1414*	0.40	siltite, medium lithified, greenish-white
	49bs	71	1471*	>1.50	siltite, well lithified, grayish-green
	38bs	115	1515*	5.00	siltite, well lithified, green
	43bs	151	1551*	10-15	siltite, well lithified, grayish-green
Goleşti	20vg	78	263	0.08	rudite, well lithified, greenish-gray
	49vg	83	268	2.50	arenite, medium lithified, grayish-white
	47vg	96	281	0.40	arenite, well lithified, white
	31vg	118	303	0.20	arenite, weakly lithified, white
*calculated considering the maximum thickness of the synclinal filling deposits (1400 m)					

3. RESULTS

3.1. Petrographic features

Table 1 reports the sample position within the sedimentological column, layer thickness, color and litification degree. Samples from both SL and GO are siltitic to arenitic, while their colors are greenish and white, respectively. The preserved volcanic texture allows to define them as vitroclastic tuffs. The superimposed epiclastic material consists both of crystalloclastes (quartz, plagioclase, biotite, muscovite) and lithoclastes (metamorphic rocks with quartz, quartz-muscovite-biotite). On the basis of optical microscope observations on 25 samples from SL and 40 from GO (data not shown), the volcanic glass appears to be nearly entirely and partially transformed at SL and GO, respectively.

3.2. Chemical composition of bulk samples

Major and trace element contents in the analyzed samples are reported in Tables 2a and 2b. Due to element mobility during the sedimentary processes, only some classification schemes of volcanic rocks may be applied to this study. According to the diagram of Winchester & Floyd (1977) that uses Zr, Ti, Nb, and Y (Fig. 3), most samples are distributed in the rhyolite-rhyodacite-dacite field, with some exceptions for several GO samples. The use of this diagram has some limitations, however, because of the mobility of several elements, frequently considered as "immobile". In fact, the experimental study carried out by Fiore et al., (1999) suggested that Y and Zr concentrations remain almost constant, while Ti and Nb continuously decrease, during a rhyolitic obsidian alteration. Therefore, sample distribution within Winchester and Floyd diagram (1977) does not only reflect the composition of volcanic glass, but also element mobility during the alteration.

Table 2a. Chemical composition (major and trace elements) of bulk samples (XRF) at Slănic.

Major oxides (%wt)	Samples			
	24bs	49bs	38bs	43bs
SiO_2	62.9	66.3	67.5	66.8
Al_2O_3	11.9	11.4	10.7	11.5
Fe_2O_3	2.6	1.0	1.1	1.2
MnO	0.0	0.0	0.0	0.0
MgO	0.9	0.7	0.4	0.7
CaO	4.6	3.6	2.9	3.3
Na_2O	0.4	2.5	2.1	2.7
K_2O	1.8	2.1	2.7	2.1
TiO_2	0.2	0.2	0.1	0.2
P_2O_5	0.1	0.0	0.1	0.1
LOI	14.9	12.9	13.1	11.8
Total	100.1	100.7	100.7	100.4
	Trace elements (mg kg^{-1})			
Ni	4	5	2	3
Zn	51	25	14	20
Ga	16	13	13	13
Rb	78	64	93	58
Sr	1338	481	445	472
Y	43	31	19	31
Zr	135	134	134	147
Nb	11	12	14	13
Pb	76	21	5	27
Th	11	11	12	11
U	<3.0	<3.0	<3.0	<3.0
Sn	5	<3.0	<3.0	<3.0
Ba	353	489	751	630
Cs	40	16	21	19
Ce	249	135	152	133

Another explanation for this distribution could be attributed to the epiclastic material.

Table 2b. Chemical composition (major and trace elements) of bulk samples (XRF) at Goleşti.

Major oxides (%wt)	Samples			
	20vg	49vg	47vg	31vg
SiO_2	47.6	58.1	58.3	67.2
Al_2O_3	12.5	13.1	11.5	12.6
Fe_2O_3	4.5	2.7	2.6	1.2
MnO	0.2	0.1	0.1	0.0
MgO	2.0	0.8	0.9	0.8
CaO	12.7	6.1	7.2	2.0
Na_2O	1.0	2.5	1.9	3.0
K_2O	2.3	3.6	3.1	1.6
TiO_2	0.6	0.2	0.2	0.2
P_2O_5	0.1	0.1	0.1	0.0
LOI	17.7	6.9	7.0	11.3
Total	101.0	94.1	92.8	99.9
	Trace elements (mg kg^{-1})			
Ni	40	13	16	4
Zn	73	59	44	29
Ga	15	16	15	14
Rb	115	163	112	77
Sr	383	240	230	366
Y	19	29	30	28
Zr	131	233	102	175
Nb	12	42	13	17
Pb	26	24	20	13
Th	5	27	12	13
U	6	7	<3.0	3
Sn	3	3	7	<3.0
Ba	445	639	590	887
Cs	20	25	12	17
Ce	100	170	81	117

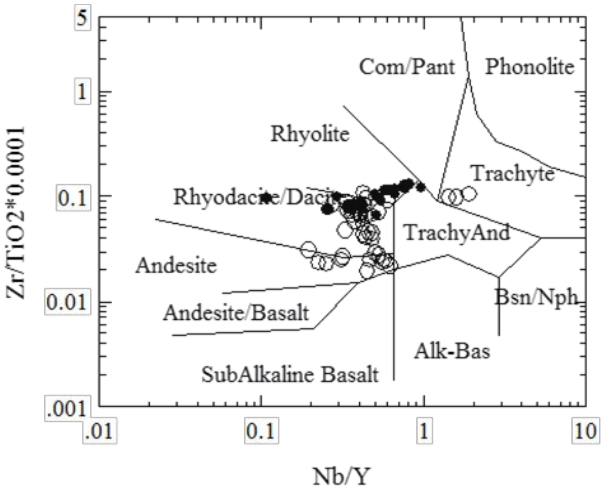

Figure 3. Samples plot within diagram of rock classifications of Winchester & Floyd (1977) (black circles - SL, open circles - GO).

3.3. Mineralogical composition of bulk samples

The mineralogical composition of samples from both deposits (Table 3) is rich and complex, thus some XRD identification challenges arise because of reflection overlapping. The most important issue was due to clinoptilolite, which shows many intense reflections that overlap those of other minerals, particularly feldspars. Nevertheless, both volcanic tuffs undoubtedly contain clay minerals, clinoptilolite, SiO_2 polymorphs and carbonates as secondary phases, formed by glass alteration. In some samples, authigenic feldspars (albite α) also occurred. Volcanic and authigenic K feldspars might also have been present, but their reflections would have been overlapped by those of clinoptilolite. As far as SiO_2 phases are concerned, it was not possible to indicate if quartz α was authigenic or epiclastic.

Table 3. Mineralogical composition of bulk samples (X-ray powder diffraction).

Samples	Minerals
Slănic	
24bs	clay minerals, clinoptilolite, opal-CT, calcite, dolomite
49bs	clay minerals, micas, clinoptilolite, quartz α, opal-CT, calcite, dolomite
38bs	clay minerals, micas, clinoptilolite, albite α, opal-CT, dolomite
43bs	clay minerals, micas, clinoptilolite, quartz α, albite β, calcite, dolomite
Goleşti	
20vg	clay minerals, micas, clinoptilolite, quartz α, albite α, calcite
49vg	clay minerals, micas, quartz α, albite α±β, calcite
47vg	clays, micas, clinoptilolite, quartz α, opal-CT, calcite
31vg	clay minerals, micas, clinoptilolite, quartz α, albite α+β, calcite

Some remarks must be made on the two groups of samples:

i) Clinoptilolite was present in all 25 samples from SL and appeared to be dominant with respect to clay minerals, which occured only in some samples. At GO, clinoptilolite occurred only in part of the 40 analyzed samples, while clay minerals were always present. This relationship was confirmed also in the eight selected samples.

ii) As far as SiO_2 phases are regarded, opal-CT occurred as authigenic phase at SL and GO only in three and one sample, respectively.

iii) Carbonates are represented by calcite at GO, and by dolomite at SL, with or without calcite.

3.4. Mineralogical composition of the <0.2 μm fraction

Table 4 summarizes the mineralogical composition of the <0.2 μm fraction whose

complexity gave rise to some issues of mineral identification, particularly due to interferences. Therefore, a specific discussion will be devoted to the characterization of each mineral group.

Table 4. Mineralogical composition of the <0.2 μm fraction.

Sample	Clay minerals	Zeolites	Alkali feldspars	SiO_2 phases
Slănic				
24bs	illite[a] smectite[b]	clinoptilolite	alkali feldspar	± quartz α ± opal-CT
49bs	illite smectite kaolinite	clinoptilolite	albite, K-feldspar	opal-CT, quartz α
38bs	illite smectite	clinoptilolite	K-feldspar ± albite	opal-CT ± quartz α
43bs	illite smectite kaolinite	clinoptilolite	albite, K-feldspar	quartz α ± opal-CT
Goleşti				
20vg	illite smectite kaolinite	clinoptilolite (low amount)	albite ± K-feldspar	no or very low
49vg	illite smectite kaolinite	clinoptilolite (very low amount)	albite ± K-feldspar	quartz α
47vg	illite smectite kaolinite	clinoptilolite (low amount)	albite ± K-feldspar	opal-CT
31vg	illite smectite kaolinite	clinoptilolite	albite, K-feldspar	no or very low

[a] pure illite (100% non-expanding material) and highly illitic mixed-layer illite/smectites (Środoń 1984)
[b] pure smectite and smectite-dominated mixed-layer illite/smectites.

The identification of coexisting smectite and illite minerals was performed following the methods described by Środoń (1981, 1984). Despite the interferences with other minerals (clinoptilolite and alkali feldspars), the results of these procedures can nevertheless provide valuable information on the presence and type of mixed-layer illite/smectites. However, the peak of clinoptilolite appeared very strong in samples 38bs, 43bs, and 49bs from SL (Fig. 4a), while only a slight peak was observed in sample 24bs from SL and the samples from GO (Fig. 4b).

The positions of smectite material reflections at about 15-16°2θ Cu (17.4-18.6°2θ Co) and 31-32°2θ Cu (36.1-37.3°2θ Co) (Fig. 5) were used to calculate the percentage of smectite layers (%S) and the thickness of ethylene glycol-smectite complex (Fig. 6a). The %S was subsequently corrected by a ΔS value obtained by plotting %S versus intensity ratio I_I/I_{I-S} on an empirical diagram (Fig. 6b). Total smectite layers percentage was therefore obtained as follows:

$$\%S_{tot} = \%S + \Delta S \quad (1)$$

The three reflections obtained for smectite material are presented in Figure 5. Sample 38bs appears to be the most affected by the presence of clinoptilolite which potentially hinders the orientation of clay crystals. Despite this interference, the peaks of the clay minerals are presumably positioned at the middle of their highest region, thus allowing for plotting the data in the diagram of Środoń (1981) (Fig. 6a). Table 5 reports the values of %S for the 8 selected samples. In all samples clinoptilolite and alkali feldspars also affected the intensity of reflections (I_I and I_{I-S}). Although the ratio I_I/I_{I-S} could not be exactly calculated, it was still possible to indicate a variation interval of ΔS using Środoń's diagram (Fig. 6b), because at a given value of %S, ΔS cannot be higher than a maximum value. Consequently, we were also able to estimate an interval for $\%S_{tot}$ (Table 5).

Table 5. Results of the R0 illite/smectite identification.

Samples		%S	Estimated $\%S_{tot}$
Goleşti	20vg	73.5	73-88
	49vg	84.6	84-96
	47vg	90.0	90-100
	31vg	95.9	96-100
Slănic	24bs	93.8	94-100
	49bs	72.1	72-85
	38bs	?	?
	43bs	75.0	75-87

The method of Środoń (1984) allows for the detection of the presence and type of some mixed-layer illite with R1 or R3 ordering, respectively and, under specific conditions, the quantification of the percent of smectite layers. This is particularly favorable for an illite-dominated illite/smectite spectrum, where characteristic mixture reflections occur at about 6-8°2θ Cu (6.9-9.3°2θ Co) and 33-35°2θ Cu (38.5-40.9°2θ Co). For the samples from SL and GO, in the region of 6-8°2θ Cu (6.9-9.3°2θ Co), only the R0 illite/smectite reflection was observed (Fig. 7 (a) and (c)). At about 33-35°2θ Cu (38.5-40.9°2θ Co), many reflections of clinoptilolite, alkali feldspars, and SiO_2 phases appeared (Fig. 7 (b) and (d)), which complicated the diffraction pattern. Except for 004 reflection of illite, in this situation it is difficult to detect if there are other reflections from illite material.

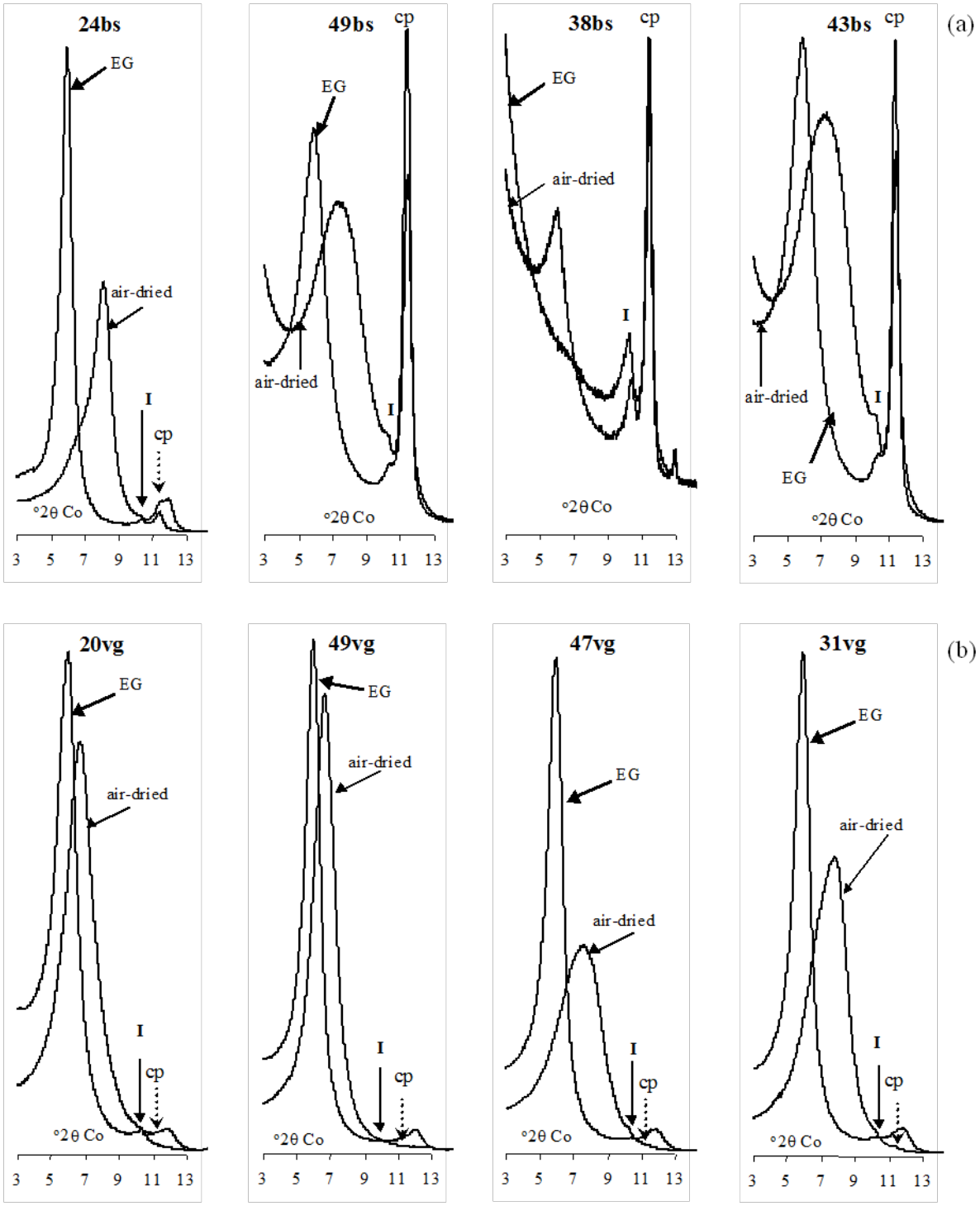

Figure 4. Highest intensity reflections of smectite material, illite material and clinoptilolite (Na-exchanged smples, CoKα radiation) (I=illite material, cp=clinoptilolite). (a) Slănic; (b) Goleşti.

Środoń's method gives further criteria to distinguish between R1 and R3 ordering in illite/smectite samples. In our case, two of the criteria proposed by Środoń (1984) may be used, namely the BB1 and BB2 values. BB1 is the joint breadth of the 001 illite and adjacent illite/smectite reflections, measured in °2θ from the point where the tails of the peak join the X-ray background; BB2 represents the joint breadth of 004 illite and adjacent illite/smectite reflections, measured in the same manner as BB1.

If BB1 and BB2>4°2θ Cu (4.64°2θ Co), the illite material is a mixture of illite and R1 illite/smectite with 15-50% smectite layers. If BB1 and BB2 <4°2θ Cu (4.64°2θ Co), the illite material is composed of pure illite (when $I_I/I_{I-S}=1$) or a mixture of illite and R3 illite/smectite with <15% smectite layers (when $I_I/I_{I-S}>1$).

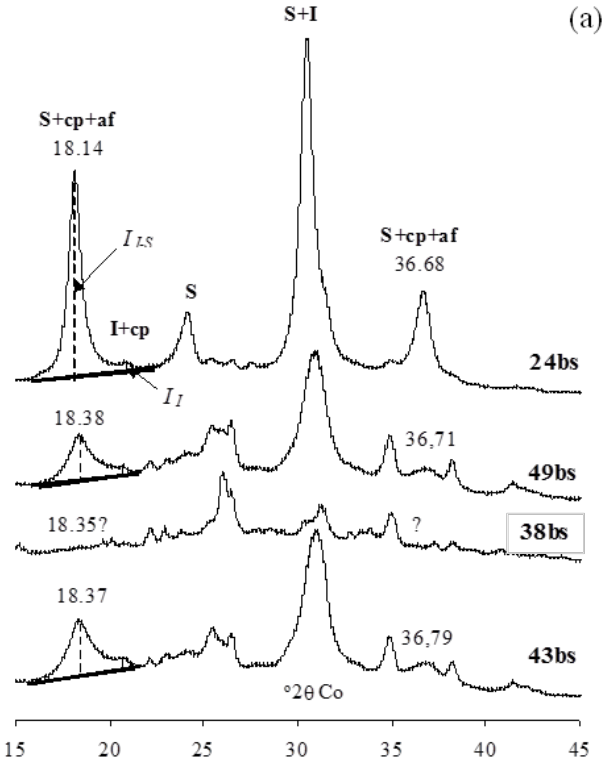

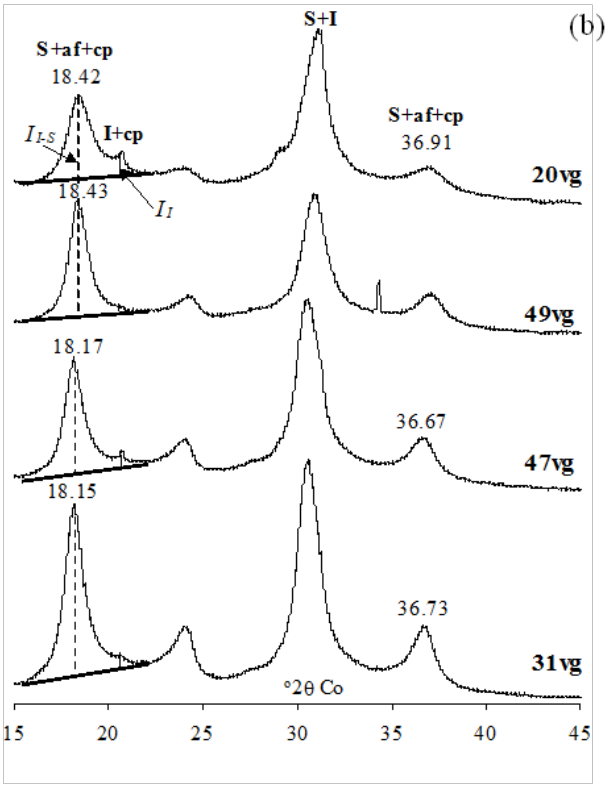

Figure 5. Position of the smectite material reflections and I_I and I_{I-S} values used to calculate the smectite layers percentage (%S) and ΔS (correction for %S), respectively, for R0 illite/smectite. Glycolated Na-exchanged samples: (a) Slănic, (b) Goleşti. (I=illite material, S=smectite material, cp=clinoptilolite, af=alkali feldspars).

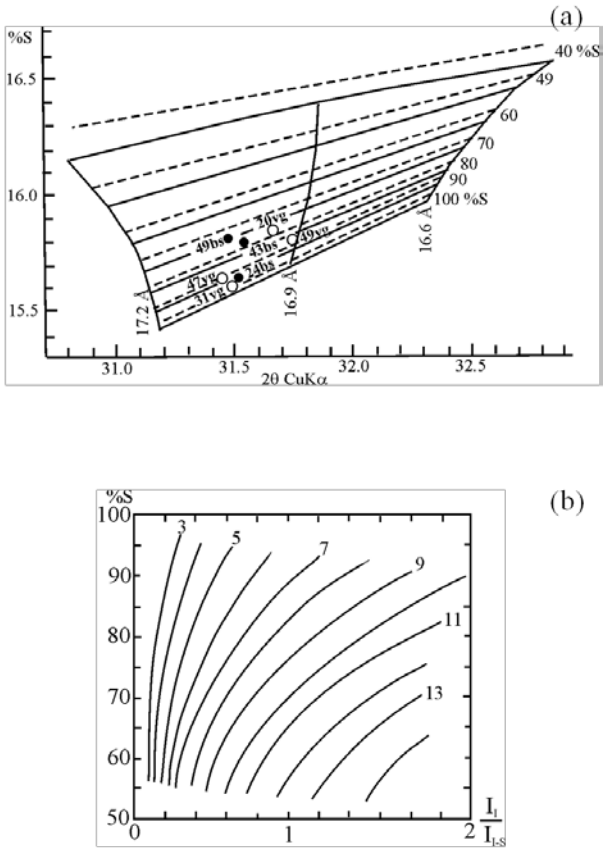

Figure 6. Plot of the samples on the diagrams of Środoń (1981): (a) Computer-calculated plot for measuring percent smectite (%S) (solid lines=1-8 layers domain size, dashed lines=1-14 layers domain size, steep curved lines=selected thicknesses of ethylene glycol-smectite complex); (b) Empirical plot for correcting %S.

Figure 7 shows the BB1 and BB2 values. While BB1 can be measured, being lower than 4.64°2θ Co, BB2 cannot be exactly estimated due to the presence of clinoptilolite and alkali feldspars. Nevertheless, it may be assumed that BB2 is not higher than the graphic representation, therefore BB2<4.64°2θ Co may also be accepted. Because it is not possible to calculate Ir, the illite material of GO and SL samples may be pure illite or a mixture of illite and R3 illite/smectite with <15% smectite layers.

The identification of alkali feldspars and SiO_2 phases was less precise for some samples (Tabs. 3 and 4) and/or phases because of their preferential orientation. Moreover, in the clinoptilolite-rich samples, its reflections overlap some of the feldspars. The presence of clinoptilolite, even in small amounts, was easily identified because of its numerous reflections (Gottardi & Galli, 1985). In addition, the heating treatment at 550 °C for 1 hour allowed to differentiate iron-rich chlorite from kaolinite (Moore & Reynolds Jr., 1997).

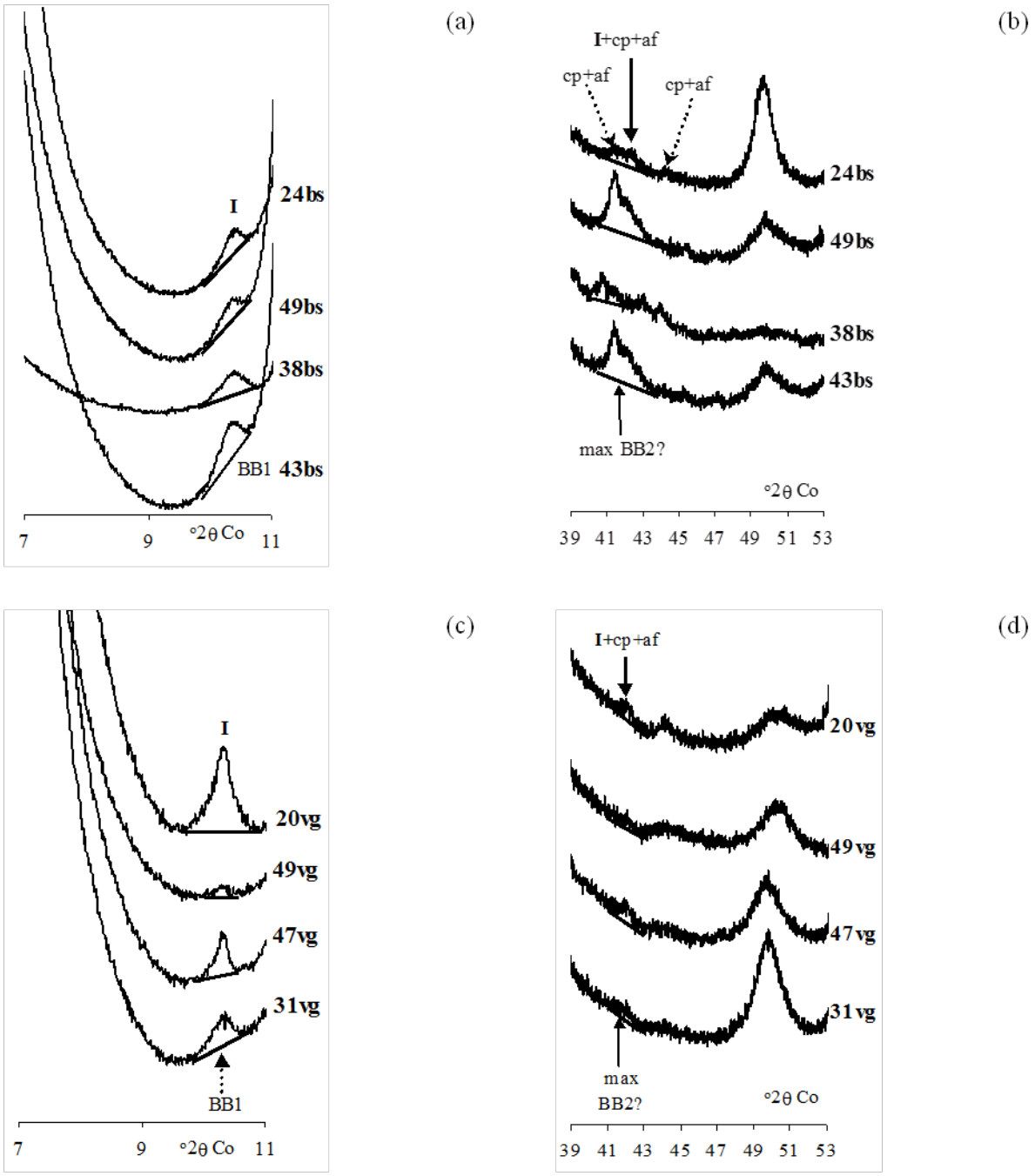

Figure 7. BB1 and BB2 parameters used to distinguish between the types of interstratification for illite-dominated minerals, after Środoń (1984). Glycolated Na-exchanged samples: (a) and (b) Slănic; (c) and (d) Goleşti. (I=illite material, S=smectite material, cp=clinoptilolite, af=alkali feldspars).

4. DISCUSSION AND CONCLUSIONS

The results obtained for the two volcanic tuffs may be classified in two groups: i) general information concerning the geological and petro-chemical features of bulk samples, and ii) mineralogical composition of the authigenic phases. Our discussion will focus on the second group of results, using the first one to define the environmental conditions of the authigenesis.

The general geological conditions revealed that the two deposits had a similar chemical composition, leading to rhyolitic-rhyodacitic-dacitic tuffs. The conditions concerning the type of explosion and the depositional process appeared to be different: at SL the explosion was subaerian, while at GO the explosion was probably submarine or phreato-magmatic, involving the participation of the solution immediately after the eruption. In both cases the volcanic glass was placed in the final depositional stage in a marine environment, then buried by more recent sediments. Because of

erosion, it was not possible to give an exact estimation of the burial depth for each layer, but in the present sedimentary column the SL tuffs appear at a greater depth than the GO ones.

In the mineralogical composition of the bulk sample and of the <0.2 μm fraction (Tabs. 3, 4 and 5, Fig. 4), the main differences were more evident in the second group of results. In fact, even if both deposits generally had the same secondary mineral assemblage, *i.e.* kaolinite, R0 illite/smectite, illite, clinoptilolite, alkali feldspars, SiO_2 phases and carbonates, the following specific features arised:

i) At SL (except for sample 24bs) the amount of clinoptilolite was higher than clay minerals, while at GO the ratio was inverted. Furthermore, in the finest fraction at GO, clinoptilolite content appeared higher within the deepest sample (31vg).

ii) As far as clay minerals are concerned, all samples contained illite and R0 illite/smectite, but kaolinite was missing in two samples from SL and its presence did not depend on depth. The smectite layers percentage of R0 illite/smectite lied between 72 and 100% (Table 5) in both sample groups. At SL this percentage seemed to be normally related to the presence of clinoptilolite, namely within the upper sample (24bs) where the maximum %S value and the minimum clinoptilolite amounts were observed; within the deeper samples, the %S decreased and clinoptilolite amount increased. At GO we observed an interesting, inverse ratio between %S and depth: the mix-layered mineral was richer in smectite as depth increased. Moreover, the deepest sample (31vg) with more clinoptilolite contained also the most smectitic R0 illite/smectite.

iii) No significant distribution of the authigenic feldspars and SiO_2 phases was evidenced, even if K-feldspar seemed to occur in the samples with more clinoptilolite or at greater depth, while albite occured in all samples. The distribution of SiO_2 phases appeared irregular, mainly because the XRD reflections of quartz α were overlapped by some of the clay minerals.

iv) Regarding carbonate composition, all samples from GO contained only calcite, while at SL dolomite was the most common mineral, with or without calcite.

All these general features support the hypothesis that the two groups of mineral assemblages have been controlled by different factors during the volcanic glass alteration. Some of the possible genetic factors could be indicated.

For both deposits the general mineral assemblage, namely the kaolinite-R0 illite/smectite-illite-clinoptilolite-alkali feldspars indicates a non-equilibrium state of the systems. On this subject, according to most researchers, this mineral assemblage would reflect a sequence of crystallization which aims to equilibrium (e.g., Dibble & Tiller, 1981). The different minerals would be related to different evolution steps of the system, namely the alteration processes during volcanic glass deposition, diagenesis, and weathering.

The pH of the system is acidic due, e.g., to the presence of some acids as condensation products on the glass shards surface in the phreato-magmatic explosions (de'Gennaro et al., 2000), or to the glass hydration in the presence of seawater. Thus, in the early stage of glass alteration, the six-fold Al coordination is favored, therefore clay minerals, mainly kaolinite and smectite, will form by reorganization of the alumino-silicate network (Leggo et al., 2001). Kaolinite is thought to be the early phase, which crystallizes in the most acidic conditions and at moderate depth, evolving to more stable clay minerals or zeolites as pH and/or depth increases. In the investigated pyroclastic deposits, kaolinite coexists with R0 illite/smectite in all samples, but the relationships between clay minerals being unknown, it is uncertain if they had formed simultaneously or successively. Further limitation may be imposed by the analysis on the <0.2 μm fraction, because kaolinite usually appears in the coarser fraction. In any case, kaolinite indicates low pH conditions and its variable amount may be related either to sea level oscillations (Anjos, 1986), or to a different further evolution of the system.

As alteration progresses, kaolinite may transform into clinoptilolite and opal-CT by burial (Senkayi et al., 1987) or into illite/smectite at a temperature between 100 and 200 °C, depending on pH and K activity (Giorgetti et al., 2000).

The occurrence of R0 illite/smectite may be interpreted differently. In general, pure smectite is thought to be the first phase that formes, while illite or clinoptilolite the subsequent ones, as alteration progresses. Samples with lower percentage of smectite layers may be interpreted either as variable degrees of smectite illitization (Hower et al., 1976), or as directly formed phases. On the basis of the first model, the smectite to illite transition takes place by K incorporation in the interlayer space, followed by low compositional modifications in the tetrahedral and octahedral sites. Therefore, different smectite layers percentage of illite/smectite could reflect different evolution steps of the smectite illitization, depending on rock age, depth, or temperature (e.g., Anjos, 1986; Hower et al., 1976). Different illitization degrees could also depend on K activity in the pore fluid (e.g., Eberl & Hower, 1976; Howard & Roy, 1985; Huang et al., 1993; Inoue,

1983; Roberson & Lahann, 1981; Whitney & Northrop, 1988) or on water/rock ratio (Ahn et al., 1988; Boles & Franks, 1979; Lanson & Champion, 1991; Yau et al., 1987; Whitney, 1990). Finally, the formation of mixed-layer R0 illite/smectite has been indicated as occurring directly from volcanic glass (de la Fuente et al., 2000). In fact, even at low temperature (60 °C), only R0 illite/smectite with 75% smectite layers and no particle with smectite-layer charge were obtained by synthesis in deionized water and solutions with Na/K ratio<1.

It appears that, for all our samples, the R0 illite/smectite with 90-100% smectite layers have formed directly from glass. The phases with lower percentages of smectite layers could have formed either directly from glass, or as transition phases in the mineral sequence of the smectite illitization. Moreover, as we already noted, at GO there is an inverse relationship between the percentage of smectite layers and depth. This could be a consequence of the stronger influence of the chemical composition of the system, which controlled both the composition of the early phases and/or the distribution of other mineral phases. Thus, only the factors which have led to the present distribution could be taken into account. In the hypothesis of the direct formation of R0 illite/smectite with 75% smectite layers (de la Fuente et al., 2000), Na/K ratio could determinate this different authigenesis, namely a higher K availability could lead to a more illitic illite/smectite. If all early phases were pure smectite, a higher K availability in the further evolution of the system would induce a more intense transition from smectite to illite in some pyroclastic layers.

This evolution may be also related to the simultaneous presence of clinoptilolite and illite. In fact, in most of the experimental and natural systems, smectite precedes clinoptilolite and illite; nevertheless, all three phases could also form simultaneously, varying only as dominance (see also Dibble & Tiller, 1981). Regarding the factors controlling the crystallization sequence and the quantitative distribution of the minerals, it is probable that the early formed smectite subsequently transformed into zeolite and illite when the system became closed (solid/liquid ratio increased) and no Mg was added to the system (de'Gennaro & Colella, 1992). However, the illite crystallization was low, depending on K availability. Higher activities for K and H_4SiO_4 in pore fluids promotes the crystallization of K-rich clinoptilolite and hiders the formation of illite/smectite, because clinoptilolite has higher amounts of Si with respect to illite (Altaner & Grim, 1990; Anjos, 1986).

Considering the above studies and our results, the mineral assemblages of the two pyroclastic deposits could be controlled by chemical conditions. It may be assumed that, in the first stage, in some pyroclastic layers, pure smectite or R0 illite/smectite had formed, depending on the depositional rate. In our samples R0 illite/smectite richer in illite occurs in the thicker layers. In these layers the solid/liquid ratio was higher, lacking conditions for zeolite formation. Because of the increase in solid/liquid ratio and pH, illite and clinoptilolite formed after sediment burial. Their authigenesis was controlled by the activity of cations and silica, as well as by burial depth. In Figure 4 it may be seen that in the clinoptilolite-rich samples from SL, illite is more abundant; this association supports the important role of depth. The occurrence of dolomite in the samples from SL may also indicate a higher smectite consumption and, as a consequence, Mg availability in solution in the latest stage of diagenesis.

As a general conclusion, the two occurrences of volcanic tuffs appear to have been subjected to different glass alteration processes, even if the early stages of transformation seem to have been the same for both, as supported by the presence of kaolinite and smectite or R0 illite/smectite. Within the same pyroclastic deposit some local differences were determined by the depositional rate; this could be the reason of a different percentage of smectite layers of illite/smectite, even if some pure smectite or kaolinite have been transformed into illite/smectite.

Initially, burial depth, and subsequently the chemical composition of the glass controlled the further evolution of the two deposits. A more important occurrence of illite and clinoptilolite was observed at SL, probably due to the higher burial depth. The dominance of clinoptilolite indicates higher K and H_4SiO_4 activities (Altaner & Grim, 1990; Anjos, 1986; de'Gennaro & Collela, 1992). Comparing the two sample groups it may be noticed that the lowest sample from GO (31vg) is mineralogically similar to the upper sample from SL (24bs). These two samples may be seen as transition points between the two pyroclastic deposits. Under the hypothesis that the volcanological and early depositional factors had a minor influence, the GO tuff may be seen as the precursor of the SL one. To verify this hypothesis, further investigations, including volcanological, sedimentological and mineralogical characterisations, are necessary.

ACKNOWLEDGMENTS

The authors would like to thank Dr. Essaid Bilal, Dr. Bernard Guy, Dr. Daniel Garcia and Dr. Jean-Jacques

Truffat from SPIN Center, École Nationale des Mines, Saint Étienne (France) for the opportunity of the TEMPRA-PECO project, powder XRD and XRF analysis, and their scientific support. We would also like to thank Dr. Cristina Panaiotu and Barbara Matei from the Department of Mineralogy, Universitatea Bucureşti (Romania), and Valentin Drăgoi from Laboratorul CCCF, Bucureşti (Romania). We thank Dr. Maria Martin and Giovanni De Luca of DISAFA, Università degli Studi di Torino (Italy) for their support in preparation of samples for XRD analysis.

REFERENCES

Ahn J.H., Peacor D.R. & Coombs D.S., 1988. *Formation mechanism of illite, chlorite and mixed-layer illite-chlorite in Triassic volcanogenic sediments from the Southland Syncline; New Zealand.* Contributions to Mineralogy and Petrology, 99, 82-89.

Altaner S.P. & Grim R.E., 1990. *Mineralogy, chemistry, and diagenesis of tuffs in the Sucker Creek Formation (Miocene), eastern Oregon.* Clays and Clay Minerals, 38, 561-572.

Amouric M. & Olives J., 1991. *Illitization of smectite as seen by high-resolution transmission electron microscopy*. European Journal of Mineralogy, 3, 831-835.

Anjos S.M.C., 1986. *Absence of clay diagenesis in Cretaceous-Tertiary marine shales, Campos Basin, Brazil.* Clays and Clay Minerals, 34, 424-434.

Balint R., Popescu I. & Ajmone-Marsan F., 2014. *Removal of leached metals from flooded/drained contaminated soils using zeolites*, in Unsaturated Soils: Research and Applications - Proceedings of the 6th International Conference on Unsaturated Soils, 2, 1683-1688.

Barth-Wirsching U. & Höller H., 1989. *Experimental studies on zeolite formation conditions.* European Journal of Mineralogy, 1, 489-506.

Boles J.R. & Franks S.G., 1979. *Clay diagenesis in Wilcox sandstones of Southwest Tecas: Implications of smectite diagenesis in sandstone cementation.* Journal of Sedimentary Petrology, 49, 55-70.

Broxton D.E., Bish D.L. & Warren R.G., 1987. *Distribution and chemistry of diagenetic minerals at Yucca Mountain, Nye County, Nevada.* Clays and Clay Minerals, 35, 89-110.

Cerri G., Cappelletti P., Langella A. & de'Gennaro M., 2001. *Zeolitization of Oligo-Miocene volcaniclastic rocks from Logurdo (northern Sardinia, Italy).* Contributions to Mineralogy and Petrology, 140, 404-421.

Cochemé J.J., Leggo P.J., Damian G., Fulop A., Ledesert B. & Grauby O., 2003. *The mineralogy and distribution of zeolitic tuffs in the Maramures Basin, Romania*. Clays and Clay Minerals, 51, 6, 599-608.

Damian G., Damian F., Macovei G., Constantina C. & Iepure G., 2007. *Zeolitic Tuffs from Costiui zone - Maramures Basin*. Carpathian Journal of Earth and Environmental Sciences, 2, 1, 59-74.

de'Gennaro M., Colella C., Franco E. & Stanzione D., 1988. *Hydrothermal conversion of trachytic glass into zeolite. 1: Reactions with deionized water.* Neues Jahrbuch für Mineralogie, Monatshefte, 4, 149-158.

de'Gennaro M. & Colella C., 1992. *Experimental clay formation through the action of hot saline waters on volcanic glass.* Mineralogica e Petrographica Acta, 35A, 275-282.

de'Gennaro M., Colella C. & Pansini M., 1993. *Hydrothermal conversion of trachytic glass into zeolite. 2.Reactions with high-salinity waters*. Neues Jahrbuch für Mineralogie, Monatshefte, 3, 97-110.

de'Gennaro M., Cappelletti P., Langella A., Perrotta A. & Scarpati C., 2000. *Genesis of zeolites in the Neapolitan Yellow Tuff: Geological, volcanological and mineralogical evidence.* Contributions to Mineralogy and Petrology, 139, 17-35.

de la Fuente S., Cuadros J., Fiore S. & Linares J., 2000. *Electron microscopy study of volcanic tuff alteration to illite-smectite under hydrothermal conditions.* Clays and Clay Minerals, 48, 339-350.

Dibble Jr. W.E. & Tiller W.A., 1981. *Kinetic model of zeolite paragenesis in tufacceous sediments.* Clays and Clay Minerals, 29, 323-330.

Eberl D.D. & Hower J., 1976. *Kinetics of illite formation.* Geological Society of America Bulletin, 87, 1326-1330.

Fiore S., Huertas F.J., Fazaki K., Huertas F. & Linares J., 1999. *A low temperature experimental alteration of a rhyolitic obsidian.* European Journal of Mineralogy, 11, 455-469.

Gottardi G. & Galli E., 1985. *Natural zeolites,* pp.341. Springer-Verlag, Berlin.

Ghiara M.R. & Petti C., 1996. *Chemical alteration of volcanic glasses and related control by secondary minerals: experimental studies.* Aquatic Geochemistry, 1, 329-354.

Ghiara M.R., Petti C. & Lonis R., 2000. *Distribution and genesis of zeolites in Tertiary ignimbrites from Sardinia: evidence of superimposed mineralogenic processes.* in: Natural Zeolites in the Third Millennium, (C. Colella & F.A. Mumpton, editors). De Frede Editore, Napoli, Italy, 177-192.

Giorgetti G., Mata M.P. & Peacor D.R., 2000. *TEM study of the mechanism of transformation of detrital kaolinite and muscovite to illite/smectite in sediments of the Salton Sea Geothermal Field.* European Journal of Mineralogy, 12, 923-934.

Howard J.J. & Roy D.M., 1985. *Development of layer charge and kinetics of experimental smectite alteration.* Clays and Clay Minerals, 33, 81-88.

Hower J., Eslinger E.V., Hower M.E. & Pery E.A., 1976. *Mechanism of burial metamorphism of*

argillaceous sediments: 1. Mineralogical and chemical evidence. Geological Society of America Bulletin, 87, 725-737.

Huang W.L., Longo J.D. & Pevear D.R., 1993. *An experimental derived kinetic model for smectite-to-illite conversion and its use as a geothermometer*. Clays and Clay Minerals, 41, 162-177.

Inoue A., 1983. *Potassium fixation by clay minerals during hydrothermal treatment.* Clays and Clay Minerals, 31, 81-91.

Istrate G., 1980. *The nature and composition of Romanian zeolites*. Anuarul Institutului de Geologie si Geofizica, LVI, Bucuresti, 143-152.

Lanson B. & Champion D., 1991. *The I/S-to-illite reaction in the late stage diagenesis.* American Journal of Science, 291, 473-506.

Leggo P.J., Cochemé J.-J., Demant A. & Lee W.T., 2001. *The role of argillic alteration in the zeolitization of volcanic glass.* Mineralogical Magazine, 65, 653-663.

Miron G.D., Neuhoff P.S. & Amthauer G., 2012. *Low-temperature hydrothermal metamorphic mineralization of island-arc volcanics, South Apuseni mountains, Romania*. Clays and Clay Minerals, 60, 1, 1-17.

Moore D.M. & Reynolds, Jr C.R., 1997. *X-Ray diffraction and the identification and analysis of clay minerals*. Oxford University Press. 210, 233-234.

Neuhoff P.S. & Ruhl L.S., 2006. *Mechanisms and geochemical significance of Si-Al substitution in zeolite solid solutions*. Chemical Geology, 225, 3-4, 373-387.

Nimirciag R., 2012. *Heavy metals in the soils of Rodna mining area, Romania and zeolite efficiency for remediation*. Environmental Engineering and Management Journal, 11, 2, 421-426.

Pop A., Vida-Simiti I., Damian G. & Iepure G., 2012. *Removal of heavy metals from wastewater by using zeolitic tuff*. Carpathian Journal of Earth and Environmental Sciences, 7, 1, 239-248.

Rabenhorst M.C. & Wilding L.P., 1984. *Rapid method to obtain carbonate-free residues from limestone and petrocalcic materials.* Soil Science Society of America Journal, 48, 216-219.

Roberson H.E. & Lahann R.W., 1981. *Smectite to illite conversion rates: effects of solution chemistry*. Clays and Clay Minerals, 29, 129-135.

Senkayi A.L., Ming D.W., Dixon J.B. & Hossner L.R., 1987. *Kaolinite, opal-CT, and clinoptilolite in altered tuffs interbedded with lignite in the Jackson Group, Texas.* Clays and Clay Minerals, 35, 281-290.

Środoń J., 1980. *Precise identification of illite/smectite interstratifications by X-ray powder diffraction.* Clays and Clay Minerals, 28, 401-414

Środoń J., 1981. *X-ray identification of randomly interstratified illite-smectite in mixtures with discrete illite.* Clays and Clay Minerals, 16, 297-304.

Środoń J., 1984. *X-ray powder diffraction identification of illitic materials.* Clays and Clay Minerals, 32, 337-349.

Stumbea D., 2010. *Acid mine drainage-related products in Negoiul Românesc quarrying waste deposits (Călimani Mts., Romania)*. Carpathian Journal of Earth and Environmental Sciences, 5, 2, 9-18.

Whitney G., 1990. *Role of water in the smectite-to-illite reaction.* Clays and Clay Minerals, 38, 343-350.

Whitney G. & Northrop H.R., 1988. *Experimental investigations of the smectite to illite reaction: Dual reaction mechanisms and oxygen-isotope systematics.* American Mineralogist, 73, 77-90.

Winchester J.A. & Floyd P.A., 1977. *Geochemical discrimination of different magma series and their differentiation products using immobile elements.* Chemical Geology, 20, 325-343.

Yau Y.C., Peacor D.R. & Essene E.J., 1987. *Smectite-illite reactions in Salton Sea shales*. Journal of Sedimentary Petrology, 57, 335-342.

Zevenbergen C., Van Reeuwijk L.P., Bradley J.P., Bloemen P. & Comans R.N.J., 1996. *Mechanism and conditions of clay formation during natural weathering of MSWI bottom ash*. Clays and Clay Minerals, 44, 546-552.

Received at: 12. 09. 2014
Revised at: 23. 10. 2014
Accepted for publication at: 31. 10. 2014
Published online at: 13. 11. 2014